POLITECNICO DI TORINO
Repository ISTITUZIONALE

Digital light processing 3D printing of polymerizable ionic liquids towards carbon capture applications

Original
Digital light processing 3D printing of polymerizable ionic liquids towards carbon capture applications / Roppolo, I., Zanatta, M., Colucci, G., Scipione, R., Cameron, J.M., Newton, G.N., Sans, V., Chiappone, A.. - In: REACTIVE & FUNCTIONAL POLYMERS. - ISSN 1381-5148. - 202:(2024). [10.1016/j.reactfunctpolym.2024.105962]

Availability:
This version is available at: 11583/2995434 since: 2024-12-17T08:14:08Z

Publisher:
Elsevier

Published
DOI:10.1016/j.reactfunctpolym.2024.105962

Terms of use:

This article is made available under terms and conditions as specified in the corresponding bibliographic description in the repository

Publisher copyright

(Article begins on next page)

11 September 2026

Reactive and Functional Polymers 202 (2024) 105962

Contents lists available at ScienceDirect

Reactive and Functional Polymers

journal homepage: www.elsevier.com/locate/react

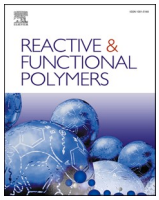

Digital light processing 3D printing of polymerizable ionic liquids towards carbon capture applications

Ignazio Roppolo [a], Marcileia Zanatta [b], Giovanna Colucci [a], Roberto Scipione [d], Jamie M. Cameron [c], Graham N. Newton [c], Victor Sans [b], Annalisa Chiappone [d,*]

[a] Dipartimento di Scienza Applicata e Tecnologia, Politecnico di Torino, C.so Duca degli Abruzzi 24, 10129 Turin, Italy
[b] Institute of Advanced Materials (INAM), Universitat Jaume I (UJI), Avenida de Vicent Sos Baynat, s/n, 12071 Castellón de la Plana, Spain
[c] Nottingham Applied Materials and Interfaces Group, School of Chemistry, University of Nottingham, Nottingham NG7 2TU, UK
[d] Dipartimento di Scienze Chimiche e Geologiche, Università di Cagliari, S.S. 554 bivio Sestu, 09042 Monserrato, Italy

ARTICLE INFO

Keywords:
Polymerizable ionic liquids
Photopolymerization
3D printing
Vat printing
Carbon capture

ABSTRACT

This study presents new 3D printable materials based on ad-hoc synthesized photocurable imidazolium ionic liquids (ILs) with bis(trifluoromethanesulfonyl)imide $(NTf_2)^-$ as counterion and two different alkyl chain's structures at the cation, with enhanced CO_2 capture properties. The molecular structure of the synthesized ILs was confirmed through NMR technique and a polymerization study was carried out, by means of photo-rheological tests and FT-IR analyses, on formulations containing a crosslinking monomer (PEGDA). The study confirmed the good reactivity of the formulations that makes them suitable for digital light processing (DLP) 3D printing technique. Simple membranes were then tested through high pressure CO_2 uptake analysis to estimate their capture efficiency, comparing the results with the standard room temperature ionic liquid (RTIL) counterpart, and evidencing an increase of CO_2 absorption regardless the pressure applied. At last, complex gyroid-like structures incorporating the synthesized ILs were successfully 3D printed, showing the remarkable ability of these materials to be processed with 3D printing technology while maintaining the great CO_2 capture performances of ionic liquids. This preliminary work paves the way for the implementation of "ad-hoc" designs to create filters or devices to enhance the CO_2 capture.

1. Introduction

The abatement of greenhouse gases (GHGs), in particular carbon dioxide, from the atmosphere is of primary importance nowadays due to the global warming and climate change. [1] The reduction of CO_2 emissions is the first stringent request but, in parallel, the option to capture, store and hopefully convert the carbon emissions to products with higher value has to be pursued. Carbon capture (CC) is thus a technology that deserves deep investigation. [2,3]

A huge variety of materials are employed in many CC processes, including porous materials such as active carbons, zeolites and metal organic frameworks (MOFs), [4–6]which exploit their high surface area and high intermolecular forces with the gas, [7] and organic solvents such as amine based solvents, [8] which are used to chemically bond the CO_2 generating chemical intermediates. [9] A further class of materials widely employed in CC technology comprehends ionic liquids. [10–12] Ionic liquids and, in particular, room temperature ionic liquids (RTILs) are salts characterized by a very low vapour pressure and a low melting temperature, [13–15]which makes them highly suitable in green chemistry. Furthermore, they can be tuned by interchanging their cations and anions giving the possibility to obtain a near-infinite number of combinations with different and specific physical and chemical properties [14]. One of the useful properties of ionic liquids is their elevated gas and in particular CO_2 solubility, [16] giving the possibility to use them as solvents for CC technologies. Nevertheless, ionic liquids are characterized by high viscosity, which can cause problems related to the capture efficiency and processing. [14,17] Aiming at solving these problems, other research led to the use of supported ionic liquid membranes (SILM) for CO_2 capture and

Abbreviations: PIL-1, C_4vbmim; $[NTf_2]$, 1-(4-vinylbenzyl)-2-methyl-3-butylimidazolium bis(trifluoromethane sulfonyl) imide; PIL-2, $(CH_3)_2C_4$vbmim; $[NTf_2]$, 1-(4-vinylbenzyl)-2-methyl-3-3,3-dimethylbutylimidazolium bis(trifluoromethanesulfonyl)imide; PEGDA, polyethylene glycol diacrylate; BAPO, Phenylbis(2,4,6-trimethylbenzoyl)phosphine oxide.

* Corresponding author.
E-mail address: annalisa.chiappone@unica.it (A. Chiappone).

https://doi.org/10.1016/j.reactfunctpolym.2024.105962
Received 11 March 2024; Received in revised form 8 May 2024; Accepted 4 June 2024
Available online 8 June 2024
1381-5148/© 2024 The Authors. Published by Elsevier B.V. This is an open access article under the CC BY license (http://creativecommons.org/licenses/by/4.0/).

separation, [18–20] but with issues related to the inevitable ionic liquid leakage. [19] In this context, ionic liquids can be chemically modified in order to be used as reactive monomers able to generate chains structures called poly ionic liquids (PILs). As polymers, PILs are solid but they are characterized by a high processability and stability. [21,22] Furthermore, PILs show greater CO_2 solubility compared to RTILs due to their higher free volume and higher diffusivity of the gas within the matrix. [23,24] Among the modified RTILs suitable for polymerization, the chemically modified RTILs bearing vinyl or acrylic moieties can be processed through photopolymerization and its related technologies. [25] In this context, light based 3D printing technologies and, in particular, digital light processing (DLP) are extremely appealing for PILs 3D printing allowing to build 3D specific geometries in short time and with reduced material waste. [26,27]

Ionic liquids and polymerizable ionic liquids have been 3D printed exploiting different printing technologies (e.g. Fuse Filament Formation, Direct Ink Writing or Bioplotting) [28–30] and for different applications [31–33] and, in detail, PILs were used in light activated 3D printing technologies for the fabrication of crosslinked structures with different properties [26] such as thermal stability [34] and ionic conductivity, [35] photocromic and thermo-responsive abilities [36,37] or antimicrobial activity [27]. The compatibility of DLP 3D printing with commercially available ionic liquids for CO_2 capture was also investigated. [38] In this study we focus on the synthesis of ionic liquids able to be processable through DLP technique and possessing enhanced CO_2 capture ability. The synthesized ionic liquids are all imidazolium based. The high CO_2 adsorption capacity of this kind of ILs, due to a remarkable solubility, was previously reported. [39,40] Despite CO_2 is more likely to interact with the anions, it was demonstrated that increasing the length of alkyl chain in the cation can slightly increase the CO_2 solubility. [39] The influence of the presence of a linear and a branched alkyl chain attached to the cation is here also investigated. Furthermore, bis(trifluoromethanesulfonyl) imide $(NTf_2)^-$ was chosen as anion due to its good CO_2 adsorption properties. [41,42] NTf_2^- anion generally gives good CO_2 solubility with most IL cations, this is mostly attributed to the flexibility of the structure of the anion aiming at increasing free volume and decreasing the energy of cavity formation. [43] Finally, a reactive functional vinyl group was grafted by quaternization reaction of the imidazole, with the primary role of reacting through a photo induced free-radical reaction with a reactive monomer (poly (ethylene glycol) diacrylate) to obtain a cross-linked polymerized ionic liquid (PIL). The synthesized polymerizable IL bearing a branched alkyl chain was added to a photocurable acrylate monomer in different amounts and the formulation were tested for photopolymerization and 3D printing. The reactivity and CO_2 sorption behaviour of the PIL bearing a linear alkyl chain was studied and compared to the previous one showing the potential of PILs.

2. Materials and methods

2.1. Materials

2-methyl imidazole, potassium hydroxide, magnesium sulfate, 4-vinylbenzyl chloride, Lithium bis(trifluoromethylsulfonyl)imide, acetonitrile, dichloromethane, acetone, diethyl ether were purchased from Sigma Aldrich, poly ethylene glycol diacrylate (PEGDA) with average molecular weight 250 was purchased from Merck, Phenylbis(2,4,6-trimethylbenzoyl) phosphine oxide (BAPO) powder 97% purity was purchased from IGM Resins, 1-bromo-3,3-dimethylbutane, 1-Phenylazo-2-naphthol-6,8-disulfonic acid disodium salt (orange G) were purchased from Tokyo Chemical Industry.

2.2. Ionic liquid synthesis

2.2.1. PIL-1. C_4vbmim[NTf_2]

2.2.1.1. 2-methyl-3-butylimidazole. During the reaction inert atmosphere was maintained to prevent any oxidation process. The reaction steps are schematically described in Fig. 1. 6 g of 2-methylimidazole were dissolved in 90 ml of acetonitrile in a two-neck round bottom flask and stirred for 15 min. Afterwards, 8 g of potassium hydroxide were added to the solution and stirred for further 30 min. Subsequently 8 ml of 1-bromobutane (R^1) were added dropwise to the solution in argon atmosphere and stirred for 4 h at room temperature. The solvent was removed under dynamic vacuum. The compound was extracted three times in 300 ml dichloromethane and washed three times with 600 ml of distilled water. The solution was dried with anhydrous magnesium sulfate and, finally, dichloromethane was removed under dynamic vacuum.

2.2.1.2. 1-(4-vinylbenzyl)-2-methyl-3-butylimidazolium chloride (C_4vbmim [Cl]). 4.85 g of 2-methyl-3-butylimidazole and 5 ml of 4-vinylbenzyl chloride were mixed dropwise in argon atmosphere in a two-neck round bottom flask. The reaction was let stir for 7 h in dark environment and inert atmosphere. Subsequently, the crude compound was dissolved in acetone and precipitated with diethyl ether (500 ml) three times. The final powder was filtrated and the solvents evaporated under dynamic vacuum.

2.2.1.3. 1-(4-vinylbenzyl)-2-methyl-3-butylimidazolium bis(trifluoromethanesulfonyl)imide. The previously prepared C_4vbmim [Cl] and 1.2 M equivalent of Lithium bis(trifluoromethylsulfonyl)imide were dissolved in distilled water in two separate beakers. The solutions were mixed together and stirred for 30 min. The upper phase (water rich) was washed (extraction) with dichloromethane three times and mixed with the bottom phase (ionic liquid rich). The solution was washed with water three times and dried over anhydrous magnesium sulphate. Subsequently the solvent was evaporated under dynamic vacuum and a transparent oil was obtained. The process was performed in dark environment to prevent the polymerization of the ionic liquid induced by light exposure.

2.2.2. PIL-2. $(CH_3)_2C_4$vbmim[NTf_2]

2.2.2.1. 2-methyl-3-3,3-dimethylbutylimidazole. 6 g of 2-methylimidazole were dissolved in 90 ml of acetonitrile and stirred for 15 min in a two-neck round bottom flask, 8 g of potassium hydroxide were added to the solution and stirred for 30 min. Subsequently 8 ml of 1-bromo-3,3-dimethylbutane (R^2) were added dropwise to the solution in argon atmosphere and stirred for 4 h at room temperature. The solvent was removed under dynamic vacuum. The compound was extracted three times in 300 ml dichloromethane and washed three times with 600 ml of deionized water. The solution was then dried over anhydrous magnesium sulfate. Finally, dichloromethane was removed under dynamic vacuum. A yellowish oil was obtained as final compound.

2.2.2.2. 1-(4-vinylbenzyl)-2-methyl-3-3,3-dimethylbutylimidazolium chloride ($(CH_3)_2C_4$vbmim[Cl]). In a two-neck round bottom flask 4.85 g of 2-methyl-3-3,3-dimethylbutylimidazole and 5 ml of 4-vinylbenzyl chloride were mixed dropwise in argon atmosphere and dark environment. The reaction was under agitation for 7 h. Subsequently, the crude compound was dissolved in acetone and precipitated with diethyl ether (500 ml) three times. The final powder was filtrated and the solvents were evaporated under dynamic vacuum.

2.2.2.3. 1-(4-vinylbenzyl)-2-methyl-3-3,3-dimethylbutylimidazolium bis(trifluoromethanesulfonyl)imide. $(CH_3)_2C_4$vbmim[Cl] and 1.2 M equivalent

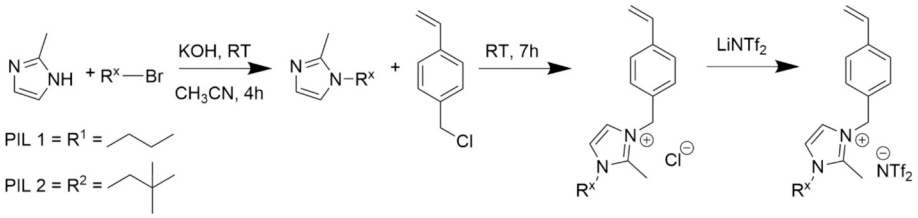

Fig. 1. Reaction steps of the two synthetized polymerizable ionic liquids.

of lithium bis(trifluoromethylsulfonyl)imide were dissolved in water in two separate beakers. The solutions were mixed together and stirred for 30 min. The upper phase (water rich) was washed (extraction) with dichloromethane three times and mixed with the bottom phase (ionic liquid rich). The solution was washed with water three times and dried over anhydrous magnesium sulphate. Subsequently the solvent was evaporated under dynamic vacuum. At the end, a transparent oil was obtained.

2.3. Formulations preparation and 3D printing

The polymerizable ionic liquid PIL-2 was mixed to PEGDA (M_w250) to obtain a set of samples with increasing concentration of PIL 40, 60, 80, 100 mol%. 1 phr (per hundred resin) of BAPO photoinitiator was added to the formulations and sonicated until its solubilization using a DU-32S ARGOLab ultrasound bath (30 kHz). 0.1 phr of Orange G was also added as a dye to improve the printing resolution.

The second ionic liquid was also mixed with PEGDA. In this case, photocurable formulations containing 80 and 100 mol% were produced and used as comparison.

The prepared formulations are listed in Table S1.

The different formulations were 3D printed using a DLP 3D printer Asiga MAX-X27 3D printer with XY pixel resolutions 27 μm and 1 μm *Z*-axis servo resolution. The LED light source is in the UV range (385 nm). During the printing an intensity of 35 mW/cm^2 and a z slice thickness of 20 μm was used. The obtained samples were then washed, gently rinsed in ethanol, and then underwent a post curing process (5 min), performed with a medium pressure mercury lamp also provided by Robotfactory equipped with a rotating platform (intensity 10 mW/cm^2).

2.4. Characterization

^{1}H NMR spectra were recorded on a Bruker AVX400 (400 MHz) spectrometer at ambient temperature. ^{13}C NMR spectra were recorded on a Bruker AVX400 (101 MHz) spectrometer at ambient temperature. ^{19}F NMR spectra were recorded on a Bruker AVX400 (376 MHz) spectrometer at ambient temperature. The samples were prepared by solubilizing the PIL in a deuterated (500 μl DMSO-d_6) solvent to avoid interference with the sample spectra and poured in an NMR tube. The spectra have been achieved with a probe temperature of 298 K under conditions for ^{1}H (spectral width 6400 Hz with 32 K data points and zero filled to 128 K to give a digital resolution of 0.05 Hz/pt). Chemical shifts were reported in parts per million (ppm, δ) and referenced to solvent pick: DMSO-d_6 (δ 2.5 in ^{1}H and 39.5 in ^{13}C).

FTIR-ATR spectra were collected using a Tensor 27 FTIR Spectrometer (Bruker) equipped with ATR tool, 32 scans were collected with a resolution of 4 cm^{-1} from 4000 to 400 cm^{-1}. Samples were analyzed when liquid and after different irradiation times (from 0 to 120 s). The peaks at 810 cm^{-1} and 920 cm^{-1} were followed to investigate the C=C double bond conversion of the acrylic group of PEGDA and the vinyl group of the ionic liquid, respectively. Rheological measurements were performed using an Anton Paar Rheometer (Physica MCR 302) in parallel plate mode. The viscosity of the photocurable formulation was evaluated performing shear sweep measurements at 25 °C. (Shear rate 0.1–100 s^{-1}) with a gap of 1 mm. Real-time photorheology measurements were performed using a quartz bottom plate and a Hamamatsu LC8 lamp with visible bulb and a cut-off filter below 400 nm equipped with 8 mm light guide. The gap between the two plates was set to 0.1 mm and the sample was kept at a constant temperature (25 °C); time sweep measurements were performed under constant shear frequency of 3.18 rad s^{-1} at 1% of amplitude; light was turned on after 1 min in order to stabilize the system, the test was stopped after reaching the G' plateau.

TGA were performed with a TA Instruments Q600 from 0 °C to 800 °C with a scan rate of 30 °C/min in air atmosphere.

DMA measurements were performed on 3D printed specimens (20 mm × 10 mm × 0.3 mm) with a Triton Technology TTDMA in tensile configuration. The experiments were carried out at a frequency of 1 Hz, a temperature ramp rate of 3 °C/min and a strain of 0.02 mm.

The printed samples were scanned by a 3Shape E3 3D optical scanner and compared with the CAD models. 3Shape Convice Analyzer was used to perform the comparative analysis between the 3D scan and the digital design (accuracy 0.007 mm, ISO 12836). Before analyzing deviations, the scan data and the reference model must be aligned; here the "best fit" approach was adopted. The comparative analysis is shown as a heatmap.

The CO_2 uptake measurements were performed at 25 °C, controlling pressure from 0 to 40 bar after placing the solid sample in the sealed chamber of an Hiden XEMIS intelligent gravimetric analyzer. Prior to CO_2 uptake determination, the samples were outgassed under vacuum at 250 °C overnight.

3. Results and discussion

Two imidazolium based ionic liquids were produced following the reaction steps are summarized in Fig. 1 and thoroughly described in the experimental part and in the SI. Briefly, for both the considered ILs, the first step consists of the nucleophilic substitution reaction of the imidazole and the corresponding bromoalkene (R^1 or R^2) in the presence of a base (potassium hydroxide). In the case of IL-1 a linear chain (R^1) is attached while for IL-2 a branched one (R^2) is used. The second step consists in the quaternization reaction of both compounds with 4-vinylbenzyl chloride to yield the IL monomers with chloride as counteranion. Finally, an anion metathesis between chloride and NTf_2 yield the monomers PIL-1 and PIL-2 employed in the 3D printable formulations.

The synthesized ionic liquids were analyzed by means of NMR technique to determine their molecular structure and atomic composition. ^{1}H and ^{13}C NMR were performed on the final compounds of all the reactions steps, while ^{19}F NMR was carried out on the ILs containing the NTf_2 anion after the ion exchange process.

In Fig. S1 of supporting information the ^{1}H, ^{13}C and ^{19}F NMR spectra of PIL-1 are shown. The main peaks of the groups related to the cation and anion corresponds to the desired compound, showing the success of the reaction.

The ^{1}H NMR spectrum of PIL-2 (see Fig. S2 in supporting information) is very similar to the previous one, except for the presence of a different molecular structure of the alkyl chain end.

Once the ILs were chemically characterized, reactive formulations that could be used to synthesize thermoset polymers were prepared, by mixing the reactive ILs with different amounts of the bifunctional monomer PEGDA and adding a suitable photoinitiator (BAPO); for all

the formulations a dye was also added, aiming to assure a better resolution in the printing step. [44] The viscosity of the formulations with increasing amount of PEGDA in PIL-2 was evaluated since this parameter is crucial for DLP process. Indeed, in the DLP-bottom-up approach the liquid formulation must flow to homogeneously fill the gap between the vat and the printed part to allow the building of each layer. The shear sweep measurements performed in the different formulations based on PIL-2 and different amounts of crosslinker, (Fig. 2a) showed that, while the pure ionic liquid presents a relatively high viscosity (0.63 Pa*s), the addition of the low molecular weight crosslinker reduces the viscosity of the formulation, resulting in typical values for 3D printable resins. [45] Neat PIL-1 showed slightly lower viscosity values (0.51 Pa*s) and the same trend with the addition of the crosslinker. Subsequently, the reactivity of the formulations was investigated by means of photo-rheology and FTIR analyses. The former analyses were carried out by irradiating the PIL-2 based liquid formulations while recording the change of the storage modulus. Fig. 2b shows the photo-rheology curves of the PIL-2-PEGDA prepared formulations (Table S1). The light was turned on after 60 s from the start of the experiment to stabilize the system and, after few seconds the storage modulus started to increase due to the crosslinking reaction. All the curves follow a high kinetic path in the first seconds of irradiation with a sharp increase of the curve. A delay in the starting of the crosslinking is visible when the amount of monofunctional PIL is increased in the formulation. Nevertheless, for all the formulations, the storage modulus reaches its maximum within the first 30 s of irradiation, indicating the complete polymerization of the samples. This analysis shows the fast reactivity of the formulations. Sample PIL-1-80 tested as comparison showed very similar behaviour to PIL-2-80 indicating the limited influence of the short lateral chain on the reactivity of the system; both the ionic liquids can be considered good candidates to be used for 3D printing in a DLP apparatus.

To further investigate the reactivity of the ionic liquids and the prepared formulations, a FTIR kinetic analysis was carried out on formulations containing 80 mol% of ionic liquid and 20 mol% of PEGDA at different irradiation times. Fig. 3 shows the FTIR-ATR spectra of the samples with the two ionic liquid after 0, 10, 20, 40, 60 and 120 s of UV light exposure. The peaks at 810 cm^{-1} and 920 cm^{-1} were followed to investigate the C═C double bond conversion of the acrylic group of PEGDA and the vinyl group of the ionic liquid, respectively. [46] For both the ionic liquids studied, the kinetic shows a decrease of the peaks related to the acrylic group of PEGDA and the vinyl group of the ionic liquids by increasing the irradiation time. The degree of conversion of the C═C double bond of both groups increases very quickly up to 80% after 20 s of exposure and reaches a total conversion after 60 s, confirming the copolymerization between PEGDA and the ionic liquids. In Table 1 the values of conversion after 120 s of the acrylic and the vinyl groups for formulations containing both ionic liquids at 80 mol% are reported.

The FTIR spectra obtained for different concentrations of PIL-2 are reported in Fig. S3.

Subsequently, the formulations were tested with for DLP 3D printing. Initially, flat membranes were printed to investigate the optimal parameters and to prepare solid samples to analyse. TGA analyses were performed on the printed samples containing 80% of both ionic liquids to investigate their thermal stability and degradation temperature. Fig. S4 in the supporting information shows the TGA curves of the samples containing the two ionic liquids. Results show the loss of weight during the heating cycles from 25 °C up to 800 °C. The samples show high thermal stability up to 350 °C where they start to degrade in two steps, with onset temperatures at 400 °C and 530 °C.

The produced samples were also tested with DMA in order to evaluate thermomechanical properties and their T_g values. Tanδ curves (Fig. 4a), as a function of temperature, show that the presence of the branched ionic liquid has multiple effects. PEGDA has a large tanδ peak centred around 45 °C (i.e. the T_g of the matrix). The presence of low amount of ILs induces a shift of the peak towards higher temperatures (the

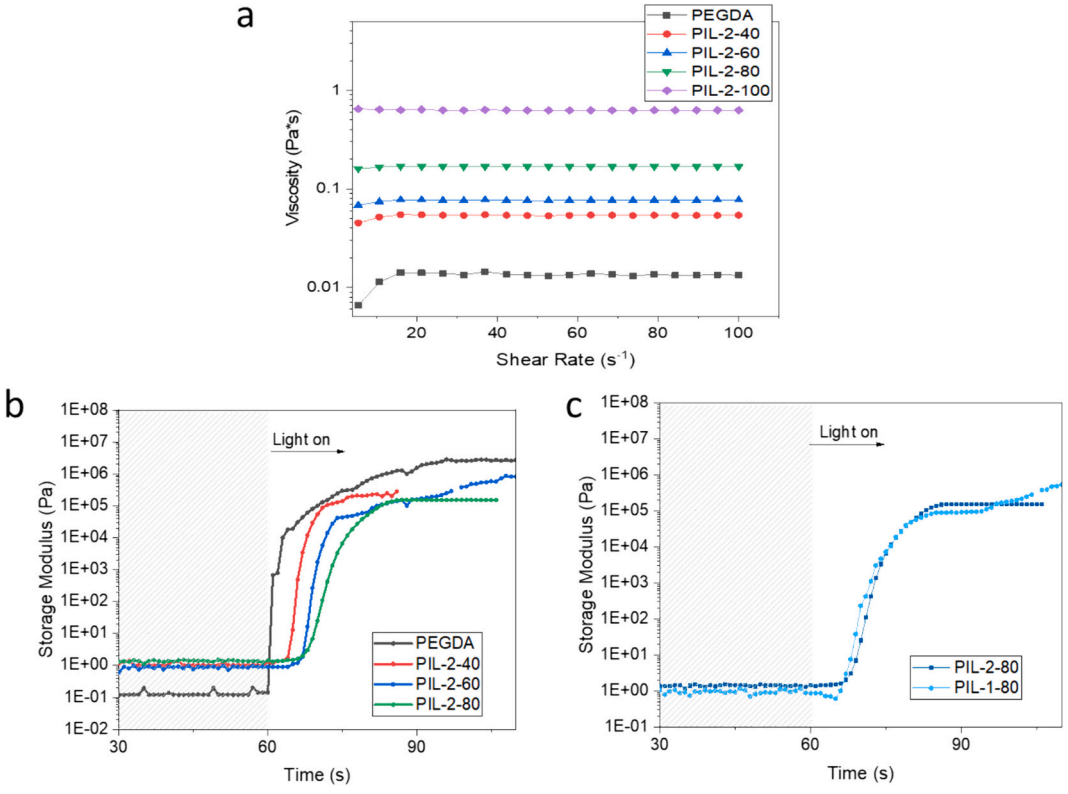

Fig. 2. a) Viscosity of the formulations containing different amounts of PIL-2. b) Photo-rheology analysis of the formulations containing different amounts of PIL-2. c) Comparison of the formulation (80:20) for the two ionic liquids (C). Light is turned on after 1 min.

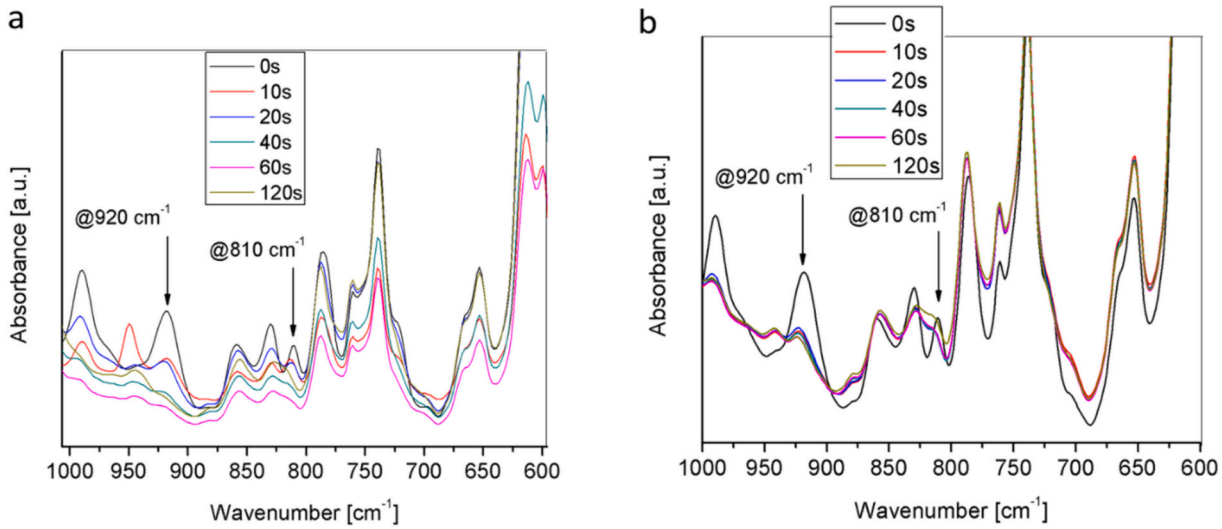

Fig. 3. FTIR-ATR analysis of: a) PIL-1 and b) PIL-2at 80/20 mol% IL/PEGDA ratio.

Table 1
Degrees of conversion of acrylic group (@ 810 cm^{-1}) and vinyl group (@920 cm^{-1}) in formulations containing 80 mol% of PIL-1 and PIL-2.

Functional group (80 mol%)	Degree of conversion (%) @ 810 cm^{-1}	Degree of conversion (%) @ 920 cm^{-1}
PIL-1	98	98
PIL-2	93	95

T_g of PIL-2-40 is about 65 °C). Increasing the amount of ILs the glass transition temperature value decreases towards lower temperatures (55 °C for PIL-2-60, 45 °C for PIL-2-80). More interestingly, the shape of tanδ dramatically changes. While PEGDA shows a very broad and flat curve, increasing the amount of ILs it is possible to observe thinner and higher curves. According to the literature, [47,48] this result indicates that the formed networks are more homogeneous and with lower crosslinking density if compared to neat PEGDA. This is in good agreement with the presence of monofunctional photocurable monomers as ILs.

Beside the printing of flat samples, the 3D printing of complex geometries was then studied: this requires the deep study of the printing parameters such as the layer thickness and the exposure times. Those parameters are strictly related to the formulation composition such as concentration of the dye, reactive monomers and fillers that indeed influence its viscosity and reactivity and also the mechanical properties of the built object.

The formulations containing 20 mol% of PEGDA with both ILs were firstly tested for the production of 3D hollow grids: both the ionic liquids allowed the printing of grids with hollow parts and good dimension fidelity to the CAD original file (see Fig. S5). This kind of geometry can be defined as 2.5 D since the same pattern is built in each layer. More complex gyroid structures were then realized with the PIL-2 at different concentrations (Fig. 4 e, f). In this case the optimization of the parameters was crucial to obtain the 3D structures. In particular, the burn-in time was chosen, after multiple tests, to achieve the best adherence without overpolymerization of the first layers, while the exposure time was adjusted to guarantee the printing precision and correct rigidity of the structure.

In all the cases the gyroid pattern was printed, nevertheless the formulation PIL-2-80 is characterized by higher viscosity and slower formation of the crosslinked network, which result in lower mechanical properties of the printed polymer for relatively short irradiation times. For this reason, PIL-2-80 did not allow to obtain self-standing structures higher than 3 mm, while reducing the amount of PIL and increasing the amount of crosslinker the less viscous formulations, giving more crosslinked networks, [49] allowed the precise printing of higher structures. This was also evidenced by the comparison of the 3D scan of the printed objects with the original CAD file reported in Figs. 4d and S5; this investigation indicates the geometrical deviation from the reference model, where the red zones represent the "material-excess" and the green ones correspond to areas with good fidelity.

Finally, aiming to preliminary understand the characteristics of the developed PILs in terms of CO_2 absorption, flat membranes were tested in a CO_2 uptake gravimetric analyzer apparatus. Measurements were carried out at high pressure from 0 to 40 bar at 25 °C and the weight variation was recorded. Fig. 4b reports the CO_2 uptake values for the samples containing the two PILs (80 mol%) compared with the room temperature ionic liquid (RTIL) counterpart 1-butyl-3-methylimidazolium bis(trifluoromethylsulfonyl)imide (bmim [NTf_2]) tested from Aki et al. [41] Results show a good positive adsorption of the samples with a slightly better uptake from the linear alkyl chain PIL indicating that the two different conformation of the alkyl chain investigated do not influence too much the gas uptake capacity. Nevertheless, both PILs experienced a high CO_2 adsorption, with an uptake of 8.76 $mg_{(CO2)}/g_{(PIL)}$ at 1 bar, that is a promising result for this kind of materials.

4. Conclusion

In conclusion, this paper showed the possibility to synthesize predesigned ionic liquids characterized by specific molecular groups, which can be used to obtain certain useful mechanical or chemical properties. In particular, the ionic liquids were chosen to be suitable for undergoing photopolymerization and creating a crosslinked poly ionic liquid (PIL) with enhanced CO_2 solubility. Moreover, the ionic liquid monomers, carefully mixed with the right amount of crosslinker, dye and photoinitiator, were studied in terms of reactivity and thermomechanical properties to enable the 3D printing of complex rigid structures through digital light processing (DLP) technique.

Uptake analyses with applied pressure from 0 to 40 bar at 25 °C showed a positive adsorption trend, very similar for both ionic liquids. Furthermore, a comparison with 1-butyl-3-methylimidazolium bis(trifluoromethylsulfonyl)imide (bmim [NTf_2]) from literature showed the uptake predominance of the prepared materials. This result underlines the concrete possibility to use this kind of materials to create solid complex objects exploiting the DLP technology and couple it with their CO_2 capture ability. Future studies will be focused on the "ad/hoc" design of new PILs structures including longer side chains or groups with a different polarity that could vary the interaction with CO_2 and other gasses, maintaining appropriate features for DLP printing i.e. suitable

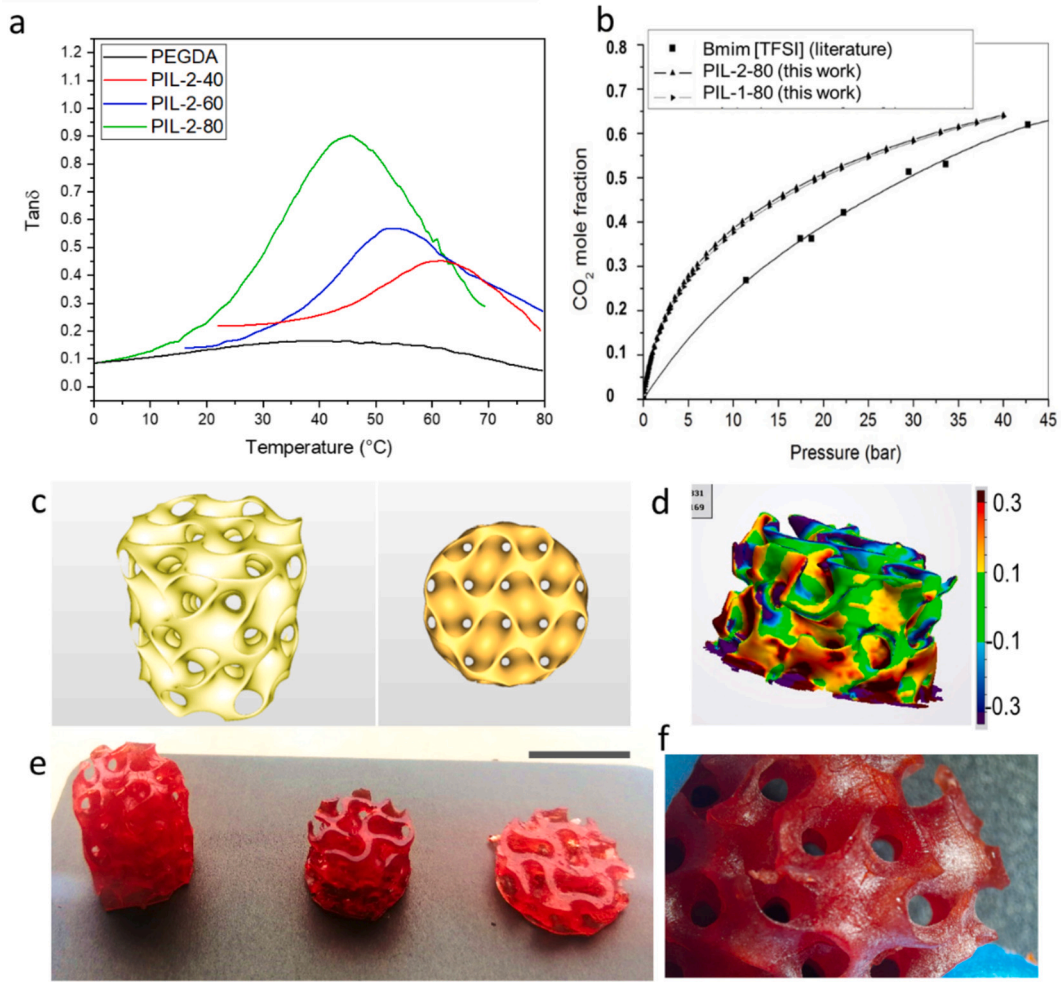

Fig. 4. a) Tanδ curves of different 3D printed samples; b) High pressure CO_2 uptake analysis for polymerized samples containing PIL-1-80 and PIL-2-80 compared to liquid counterpart 1-butyl-3-methylimidazolium bis(trifluoromethylsulfonyl)imide (bmim [NTf_2]), with applied pressure from 0 to 40 bar at 25 °C performed using gravimetric analyzer. The data of bmim [NTf_2] were fitted with a polynomial function of the fourth order; c) STL images of the gyroid structures d) color map resulting from the superimposition of the 3D scan of the gyroid printed with the formulation PIL-2-60 and its STL file. The heat map indicates the difference between the CAD model and the printed object in mm e) Printed structures with PIL-2 at different molar ratios PIL-2-40 left, PIL-2-60 middle, PIL-2-80 right (scale bar 1 cm) f) Magnification of the PIL-2-40 sample.

viscosity and reactivity aiming to merge high performing materials with the 3D virtual design of filters or devices that can further enhance the CO_2 capture.

CRediT authorship contribution statement

Ignazio Roppolo: Conceptualization, Visualization, Supervision, Writing – original draft, Funding acquisition. **Marcileia Zanatta:** Investigation, Visualization, Writing – review & editing. **Giovanna Colucci:** Investigation, Formal analysis, Funding acquisition. **Roberto Scipione:** Investigation, Formal analysis. **Jamie M. Cameron:** Investigation, Formal analysis. **Graham N. Newton:** Supervision, Writing – original draft. **Victor Sans:** Conceptualization, Methodology, Visualization, Supervision, Writing – review & editing, Funding acquisition. **Annalisa Chiappone:** Conceptualization, Methodology, Supervision, Project administration, Writing – review & editing, Funding acquisition.

Declaration of competing interest

The authors declare they have no competing financial interest or personal relastionship that could have appeared to influence the work reported in this paper.

Data availability

Data will be made available on request.

Acknowledgements

This work has been developed within the framework of the projects: 1) e.INS- Ecosystem of Innovation for Next Generation Sardinia (cod. ECS 00000038) funded by the Italian Ministry for Research and Education (MUR) under the National Recovery and Resilience Plan (NRRP) - MISSION 4 COMPONENT 2, "From research to business" INVESTMENT 1.5, "Creation and strengthening of Ecosystems of innovation" and construction of "Territorial R&D Leaders". 2) TED2021-130288B-I00 funded by the MICIN/AEI/10.13039/501100011033 Unión Europea NextGenerationEU/ PRTR. Generalitat Valenciana is gratefully acknowledged for funding (CIDEGENT 2018/036).

3) Finally, the work of I.R. and G.C. was carried out within the Ministerial Decree no. 1062/2021 and received funding from the FSE REACT-EU - PON Ricerca e Innovazione 2014–2020. This manuscript reflects only the authors' views and opinions, neither the European Union nor the European Commission can be considered responsible for them.

Appendix A. Supplementary data

Supplementary data to this article can be found online at https://doi.org/10.1016/j.reactfunctpolym.2024.105962.

References

[1] J.C.T. Bieser, R. Hintemann, L.M. Hilty, S. Beucker, A review of assessments of the greenhouse gas footprint and abatement potential of information and communication technology, Environ. Impact Assess. Rev. 99 (Mar. 01, 2023), https://doi.org/10.1016/j.eiar.2022.107033. Elsevier Inc.

[2] M. Yusuf, H. Ibrahim, A comprehensive review on recent trends in carbon capture, utilization, and storage techniques, J. Environ. Chem. Eng. 11 (6) (Dec. 01, 2023), https://doi.org/10.1016/j.jece.2023.111393. Elsevier Ltd.

[3] H. McLaughlin, et al., Carbon capture utilization and storage in review: sociotechnical implications for a carbon reliant world, Renew. Sust. Energ. Rev. 177 (May 01, 2023), https://doi.org/10.1016/j.rser.2023.113215. Elsevier Ltd.

[4] D.G. Boer, J. Langerak, P.P. Pescarmona, Zeolites as selective adsorbents for CO2 separation, ACS Appl. Energy Mater. 6 (5) (Mar. 13, 2023) 2634–2656, https://doi.org/10.1021/acsaem.2c03605. American Chemical Society.

[5] S.K. Gebremariam, L.F. Dumée, P.L. Llewellyn, Y.F. Alwahedi, G.N. Karanikolos, Metal-organic framework hybrid adsorbents for carbon capture - a review, J. Environ. Chem. Eng. 11 (2) (Apr. 01, 2023), https://doi.org/10.1016/j.jece.2023.109291. Elsevier Ltd.

[6] J. Serafin, B. Dziejarski, Activated carbons—preparation, characterization and their application in CO2 capture: a review, Environ. Sci. Pollut. Res. (2023), https://doi.org/10.1007/s11356-023-28023-9.

[7] A. Rajendran, G.K.H. Shimizu, T.K. Woo, The challenge of water competition in physical adsorption of CO2 by porous solids for carbon capture applications – a short perspective, Adv. Mater. (2023), https://doi.org/10.1002/adma.202301730.

[8] Z. (Henry) Liang, et al., Recent progress and new developments in post-combustion carbon-capture technology with amine based solvents, Int. J. Greenhouse Gas Control 40 (Sep. 01, 2015) 26–54, https://doi.org/10.1016/j.ijggc.2015.06.017. Elsevier Ltd.

[9] T.N. Borhani, M. Wang, Role of solvents in CO2 capture processes: the review of selection and design methods, Renew. Sust. Energ. Rev. 114 (Oct. 01, 2019), https://doi.org/10.1016/j.rser.2019.109299. Elsevier Ltd.

[10] S. Zeng, et al., Ionic-liquid-based CO2 capture systems: structure, interaction and process, Chem. Rev. 117 (14) (Jul. 26, 2017) 9625–9673, https://doi.org/10.1021/acs.chemrev.7b00072. American Chemical Society.

[11] W. Faisal Elmobarak, F. Almomani, M. Tawalbeh, A. Al-Othman, R. Martis, K. Rasool, Current status of CO2 capture with ionic liquids: development and progress, Fuel 344 (Jul. 2023), https://doi.org/10.1016/j.fuel.2023.128102.

[12] A. Krishnan, K.P. Gopinath, D.V.N. Vo, R. Malolan, V.M. Nagarajan, J. Arun, Ionic liquids, deep eutectic solvents and liquid polymers as green solvents in carbon capture technologies: a review, Environ. Chem. Lett. 18 (6) (Nov. 01, 2020) 2031–2054, https://doi.org/10.1007/s10311-020-01057-y. Springer Science and Business Media Deutschland GmbH.

[13] Y. Pei, Y. Zhang, J. Ma, M. Fan, S. Zhang, J. Wang, Ionic liquids for advanced materials, Materials Today Nano 17 (Mar. 01, 2022), https://doi.org/10.1016/j.mtnano.2021.100159. Elsevier Ltd.

[14] S.K. Singh, A.W. Savoy, Ionic liquids synthesis and applications: an overview, J. Mol. Liq. 297 (Jan. 01, 2020), https://doi.org/10.1016/j.molliq.2019.112038. Elsevier B.V.

[15] Z. Lei, B. Chen, Y.M. Koo, D.R. Macfarlane, Introduction: ionic liquids, Chem. Rev. 117 (10) (May 24, 2017) 6633–6635, https://doi.org/10.1021/acs.chemrev.7b00246. American Chemical Society.

[16] B.R. Mellein, A.M. Scurto, M.B. Shiflett, Gas solubility in ionic liquids, Curr. Opin. Green Sustain. Chem. 28 (Apr. 01, 2021), https://doi.org/10.1016/j.cogsc.2020.100425. Elsevier B.V.

[17] K. Paduszyński, U. Domańska, Viscosity of ionic liquids: an extensive database and a new group contribution model based on a feed-forward artificial neural network, J. Chem. Inf. Model. 54 (5) (Apr. 2014) 1311–1324, https://doi.org/10.1021/ci500206u.

[18] Z. Shamair, N. Habib, M.A. Gilani, A.L. Khan, Theoretical and experimental investigation of CO2 separation from CH4 and N2 through supported ionic liquid membranes, Appl. Energy 268 (Jun. 2020), https://doi.org/10.1016/j.apenergy.2020.115016.

[19] T. Patil, S. Dharaskar, M. Sinha, S.S. Jampa, Effectiveness of ionic liquid-supported membranes for carbon dioxide capture: a review, Environ. Sci. Pollut. Res. 29 (24) (May 01, 2022) 35723–35745, https://doi.org/10.1007/s11356-022-19586-0. Springer Science and Business Media Deutschland GmbH.

[20] W.U. Mulk, et al., Breaking boundaries in CO2 capture: ionic liquid-based membrane separation for post-combustion applications, J. CO2 Util. 75 (Sep. 01, 2023), https://doi.org/10.1016/j.jcou.2023.102555. Elsevier Ltd.

[21] Y. Biswas, P. Banerjee, T.K. Mandal, From polymerizable ionic liquids to poly(ionic liquid)s: structure-dependent thermal, crystalline, conductivity, and solution thermoresponsive behaviors, Macromolecules 52 (3) (Feb. 2019) 945–958, https://doi.org/10.1021/acs.macromol.8b02351.

[22] A. Eftekhari, T. Saito, Synthesis and properties of polymerized ionic liquids, Eur. Polym. J. 90 (May 01, 2017) 245–272, https://doi.org/10.1016/j.eurpolymj.2017.03.033. Elsevier Ltd.

[23] O. Lebedeva, D. Kultin, L. Kustov, Advanced research and prospects on polymer ionic liquids: trends, potential and application, Green Chem. 25 (22) (Sep. 26, 2023) 9001–9019, https://doi.org/10.1039/d3gc02131a. Royal Society of Chemistry.

[24] S. Zulfiqar, M.I. Sarwar, D. Mecerreyes, Polymeric ionic liquids for CO2 capture and separation: potential, progress and challenges, Polym. Chem. 6 (36) (Sep. 28, 2015) 6435–6451, https://doi.org/10.1039/c5py00842e. Royal Society of Chemistry.

[25] V. Strehmel, P.I. Kaestner, B. Strehmel, Synthesis and photoinitiated polymerization of new ionic liquid methacrylates, J. Polym. Sci. 61 (3) (Jan. 2023) 234–250, https://doi.org/10.1002/pol.20220361.

[26] S. Miralles-Comins, M. Zanatta, V. Sans, Advanced formulations based on poly (ionic liquid) materials for additive manufacturing, Polymers 14 (23) (Dec. 01, 2022), https://doi.org/10.3390/polym14235121. MDPI.

[27] S. Miralles-Comins, et al., Development of high-resolution 3D printable polymerizable ionic liquids for antimicrobial applications, Device 2 (2) (Feb. 2024) 100224, https://doi.org/10.1016/j.device.2023.100224.

[28] X. Liu, Y. Shang, J. Zhang, C. Zhang, Ionic liquid-assisted 3D printing of self-polarized β-PVDF for flexible piezoelectric energy harvesting, ACS Appl. Mater. Interfaces 13 (12) (Mar. 2021) 14334–14341, https://doi.org/10.1021/acsami.1c03226.

[29] E. Karjalainen, et al., Tunable ionic control of polymeric films for inkjet based 3D printing, ACS Sustain. Chem. Eng. 6 (3) (Mar. 2018) 3984–3991, https://doi.org/10.1021/acssuschemeng.7b04279.

[30] M. Zhang, et al., 3D printing for biological scaffolds using poly(ionic liquid)/gelatin/sodium alginate ink, Macromol. Mater. Eng. 306 (7) (Jul. 2021), https://doi.org/10.1002/mame.202100084.

[31] K.R. Hossain, P. Jiang, X. Yao, X. Yang, D. Hu, X. Wang, Ionic liquids for 3D printing: fabrication, properties, applications, J. Ionic Liq. 3 (2) (Dec. 01, 2023), https://doi.org/10.1016/j.jil.2023.100066. Elsevier B.V.

[32] K. Sheikh, K.R. Hossain, M.A. Hossain, M.S.I. Sagar, M.R.H. Raju, F. Haque, 3D printed ionic liquids based hydrogels and applications, J. Ionic Liq. 4 (1) (Jun. 01, 2024), https://doi.org/10.1016/j.jil.2024.100093. Elsevier B.V.

[33] H. Nulwala, A. Mirjafari, X. Zhou, Ionic liquids and poly(ionic liquid)s for 3D printing – a focused mini-review, Eur. Polym. J. 108 (Nov. 01, 2018) 390–398, https://doi.org/10.1016/j.eurpolymj.2018.09.023. Elsevier Ltd.

[34] A.R. Schultz, et al., 3D printing phosphonium ionic liquid networks with mask projection microstereolithography, ACS Macro Lett. 3 (11) (Nov. 2014) 1205–1209, https://doi.org/10.1021/mz5006316.

[35] Z. Wang, J. Zhang, J. Liu, S. Hao, H. Song, J. Zhang, 3D printable, highly stretchable, superior stable ionogels based on poly(ionic liquid) with hyperbranched polymers as macro-cross-linkers for high-performance strain sensors, ACS Appl. Mater. Interfaces 13 (4) (Feb. 2021) 5614–5624, https://doi.org/10.1021/acsami.0c21121.

[36] V.F. Korolovych, et al., Thermally responsive hyperbranched poly(ionic liquid)s: assembly and phase transformations, Macromolecules 51 (13) (Jul. 2018) 4923–4937, https://doi.org/10.1021/acs.macromol.8b00845.

[37] D.J. Wales, Q. Cao, K. Kastner, E. Karjalainen, G.N. Newton, V. Sans, 3D-printable photochromic molecular materials for reversible information storage, Adv. Mater. 30 (26) (Jun. 2018), https://doi.org/10.1002/adma.201800159.

[38] M. Gillono, et al., Study on the printability through digital light processing technique of ionic liquids for CO2 capture, Polymers (Basel) 11 (12) (Dec. 2019), https://doi.org/10.3390/polym11121932.

[39] M. Zhang, R. Semiat, X. He, Recent advances in poly(ionic liquids) membranes for CO2 separation, Sep. Purif. Technol. 299 (Oct. 15, 2022), https://doi.org/10.1016/j.seppur.2022.121784. Elsevier B.V.

[40] M. Zhang, L. Chen, Z. Yuan, R. Semiat, X. He, CO2-philic imidazolium-based poly (ionic liquid) composite membranes for enhanced CO2/N2 separation, Ind. Eng. Chem. Res. 62 (22) (Jun. 2023) 8902–8910, https://doi.org/10.1021/acs.iecr.3c01083.

[41] S.N.V.K. Aki, B.R. Mellein, E.M. Saurer, J.F. Brennecke, High-Pressure Phase Behavior of Carbon Dioxide with Imidazolium-Based Ionic Liquids, 2004, https://doi.org/10.1021/jp046895.

[42] J. Zhang, et al., CO2 responsive imidazolium-type poly(ionic liquid) gels, Macromol. Rapid Commun. 37 (14) (Jan. 2016) 1194–1199, https://doi.org/10.1002/marc.201600069.

[43] Y.F. Hu, Z.C. Liu, C.M. Xu, X.M. Zhang, The molecular characteristics dominating the solubility of gases in ionic liquids, Chem. Soc. Rev. 40 (7) (Jun. 2011) 3802–3823, https://doi.org/10.1039/c0cs00006j.

[44] M. Gastaldi, et al., Functional dyes in polymeric 3D printing: applications and perspectives, ACS Mater. Lett. 3 (1) (Jan. 2021) 1–17, https://doi.org/10.1021/acsmaterialslett.0c00455.

[45] A. Cortés, et al., DLP 4D-printing of remotely, modularly, and selectively controllable shape memory polymer nanocomposites embedding carbon nanotubes, Adv. Funct. Mater. 31 (50) (Dec. 2021), https://doi.org/10.1002/adfm.202106774.

[46] G. Gonzalez, et al., A facile and green microwave-assisted strategy to induce surface properties on complex-shape polymeric 3D printed structures, Macromol. Mater. Eng. (2023), https://doi.org/10.1002/mame.202300118.

[47] A. Chiappone, et al., 3D printed PEG-based hybrid nanocomposites obtained by sol-gel technique, ACS Appl. Mater. Interfaces 8 (8) (Mar. 2016) 5627–5633, https://doi.org/10.1021/acsami.5b12578.

[48] P. Marx, et al., 3D-printing of high-κ thiol-ene resins with spiro-orthoesters as anti-shrinkage additive, Macromol. Mater. Eng. 304 (12) (Dec. 2019), https://doi.org/10.1002/mame.201900515.

[49] J. Wang, et al., All-in-one cellulose nanocrystals for 3D printing of nanocomposite hydrogels, Angew. Chem. 130 (9) (Feb. 2018) 2377–2380, https://doi.org/10.1002/ange.201710951.